



Available online at [www.sciencedirect.com](http://www.sciencedirect.com)

**ScienceDirect**



Energy Reports 9 (2023) 1764–1773

[www.elsevier.com/locate/egyr](http://www.elsevier.com/locate/egyr)

2022 International Conference on Frontiers of Energy and Environment Engineering, CFEEE  
2022, 16–18 December, 2022, Beihai, China

## Measurements and analysis of solar spectrum in near space

Guoning Xu<sup>a,b,\*<sup>1</sup></sup>, Zhijie Ke<sup>a,b,1</sup>, Chunyu Zhuang<sup>a,b,1</sup>, Yongxiang Li<sup>a,\*<sup>2</sup></sup>, Rong Cai<sup>a,b</sup>,  
Yanchu Yang<sup>a,b</sup>, Xiaowei Du<sup>a</sup>

<sup>a</sup> Aerospace Information Research Institute, Chinese Academy of Sciences, Beijing 100094, China

<sup>b</sup> University of Chinese Academy of Sciences, Beijing 100049, China

Received 4 April 2023; accepted 12 April 2023

Available online 26 April 2023

### Abstract

The experiment for measuring the solar spectrum at different latitudes and altitudes was conducted to obtain a suitable Air Mass Zero (AM0) standard solar cell calibration strategy with high altitude balloon flight calibration method. This is the world's first acquisition of solar spectrum data at an altitude of 35 km using high-altitude balloon platform. The solar spectrum at the upper boundary of the atmosphere was measured and the spectral distribution was obtained from 20 to 35 km during the ascent. The results show that spectral distribution at 35 km is almost equivalent to that of AM0, the peak irradiance at 35 km is close to that of AM0, and the highest peak of this spectrum is at 450.2 nm. Comparing the results taken at different altitude, the effect of ozone, oxygen and water vapor is clearly seen. The measurement methods and results discussed in this paper can assist in verifying the accuracy of space solar cell calibration using high-altitude balloons. It could also provide a reference for the design of photovoltaic energy systems for near space aircrafts. Finally, the results taken from the launch site may be of use for the air quality monitoring and the design of photovoltaic system used in ground-based solar power generation in the Qinghai-Tibet Plateau.

© 2023 The Authors. Published by Elsevier Ltd. This is an open access article under the CC BY-NC-ND license (<http://creativecommons.org/licenses/by-nc-nd/4.0/>).

Peer-review under responsibility of the scientific committee of the 2022 International Conference on Frontiers of Energy and Environment Engineering, CFEEE, 2022.

**Keywords:** Solar spectrum; Near space; Spectral measurement, Solar cell calibration

### 1. Introduction

The study of solar cell calibration technology is an important tool for space solar cell measurements. It is essential for a comprehensive understanding of the operating characteristics of solar cells used in space and near space. In order to provide accurate and reliable design parameters for spacecraft and near space vehicle design, precise performance data of solar cells under standard sunlight are required for designing solar cell energy systems [1]. At the present stage, solar cell calibrations are mainly operated on the ground, calibrating solar cells using light

\* Corresponding author at: Aerospace Information Research Institute, Chinese Academy of Sciences, Beijing 100094, China.

\*\* Corresponding author.

E-mail addresses: [xugn@aircas.ac.cn](mailto:xugn@aircas.ac.cn) (G. Xu), [liyx@aircas.ac.cn](mailto:liyx@aircas.ac.cn) (Y. Li).

<sup>1</sup> These authors contributed equally to this work and should be considered co-first authors.

<https://doi.org/10.1016/j.egyr.2023.04.229>

2352-4847/© 2023 The Authors. Published by Elsevier Ltd. This is an open access article under the CC BY-NC-ND license (<http://creativecommons.org/licenses/by-nc-nd/4.0/>).

Peer-review under responsibility of the scientific committee of the 2022 International Conference on Frontiers of Energy and Environment Engineering, CFEEE, 2022.

simulators [2]. Due to the difficulty of spectral reproduction, there are significant errors in the results from ground simulator calibrations, and the measurement results are not sufficient to reflect the performance of solar cells, so it is urgent to carry out research on high-altitude space solar cell calibration technology.

In the outer layer of the earth's atmosphere, the solar radiation intensity is less affected by atmospheric attenuation, which is the ideal environment for solar cell calibration tests. At present, the commonly used calibration platform for the outer atmosphere are mainly high-altitude aircrafts [3], satellites [4], rockets [5] and high-altitude balloons [6–8]. The high-altitude aircraft is relatively flexible and convenient for sun tracking, but the flight altitude is relatively low and the accuracy of calibration results is not high. Calibration using satellites and rockets can produce accurate results, but the cost is too high and it is difficult to recover tested solar cells. In contrast, the high-altitude balloon calibration method can reach an altitude of about 35 km and tested solar cells can be easily recovered. These recovered cells can be used as primary standard solar cells to calibrate other cells. The results from balloon calibration are accurate, reliable and the cost of such experiments is relatively low [9,10]. Therefore, it is of great engineering value to develop a space solar cell calibration device based on high-altitude balloons.

However, whether the solar spectrum at 35 km is consistent with the air mass zero (AM0) spectrum, what are the differences in the spectra of each band, and how these differences affect the cells to be calibrated (especially the new multi-junction cells) are key questions that affect the accuracy of the high-altitude balloon calibration results, but these questions have not been studied before.

The accurate measurement of the solar radiation spectrum is also valuable in many other fields, such as photovoltaic (PV) system design and the study of meteorology. While it is easy to measure the spectrum of solar on the ground, it is more difficult to make similar measurement at higher altitude, in space or near space conditions.

In the field of atmospheric pollution monitoring, the method of measuring the absorption spectrum of solar radiation by the atmosphere has become a thriving research topic. In order to obtain the absorption spectrum, the solar spectrum at upper atmosphere must be obtained first to provide a reference spectrum. By applying the differential absorption method, the vertical column density of atmospheric pollution gases (e.g., nitrogen dioxide, sulfur dioxide, etc.) or other atmospheric compositions that could influence the environment and require monitoring (e.g., ozone, carbon dioxide, water vapor, etc.) can be derived from the difference between the locally collected solar spectrum (sample spectrum) and reference spectrum [11–13].

To address these practical needs of solar spectral measurements in near space, we use a high-altitude balloon to send a spectral measurement system to near space, reaching an altitude of 35 km. The balloon was launched in September 2021, the launch site is in Da Qaidam, Qinghai. A multi-channel fiber-optic spectrometer was used to acquire the solar radiation spectrum at this altitude, and to measure the spectrum during the ascent and at other locations with different altitudes and locations for comparison.

## 2. Method

In order to obtain a suitable AM0 Standard solar cell calibration strategy with high altitude balloon flight calibration method, the experiments for measuring the solar spectrum at different latitudes and altitudes are taken, the flowchart of this paper is depicted as Fig. 1. Firstly, before experiment, the spectral measurement device is calibrated and the measurement ranges are determined. Then, the experiments for solar spectrum measurement at north latitudes between 28° and 37° are taken, and the altitudes are from 3 km to 35 km. Lastly, the collected solar spectrum data from the experiments are used to compare with the standard AM0 spectrum at ultraviolet band, visible band and infrared band, and AM0 Standard solar cell calibration strategy is obtained.

### 2.1. Solar spectrum measurement system

The spectral measurement system used in this experiment consists of a visible spectrometer, an RS-485 adapter board and a data storage board. The RS-485 adapter board and the data storage board form the data conversion and storage system, which is used to convert and store the spectral data collected by the spectrometer on a memory card for subsequent processing and analysis. The spectrometer is a PG2000-Pro-EX spectrometer which has a detection range of 250 nm–1100 nm. The integration time can be set according to the intensity of the solar radiation. The spectrometer is equipped with a back-illuminated Charge-coupled Device (CCD) detector, the inside of this spectrometer is coated with aerospace grade highly absorbent material. The probe is mounted at a zenith angle of 0 and fitted with a cosine corrector to enable the acquisition of the sky spectrum. Because of the use of cosine

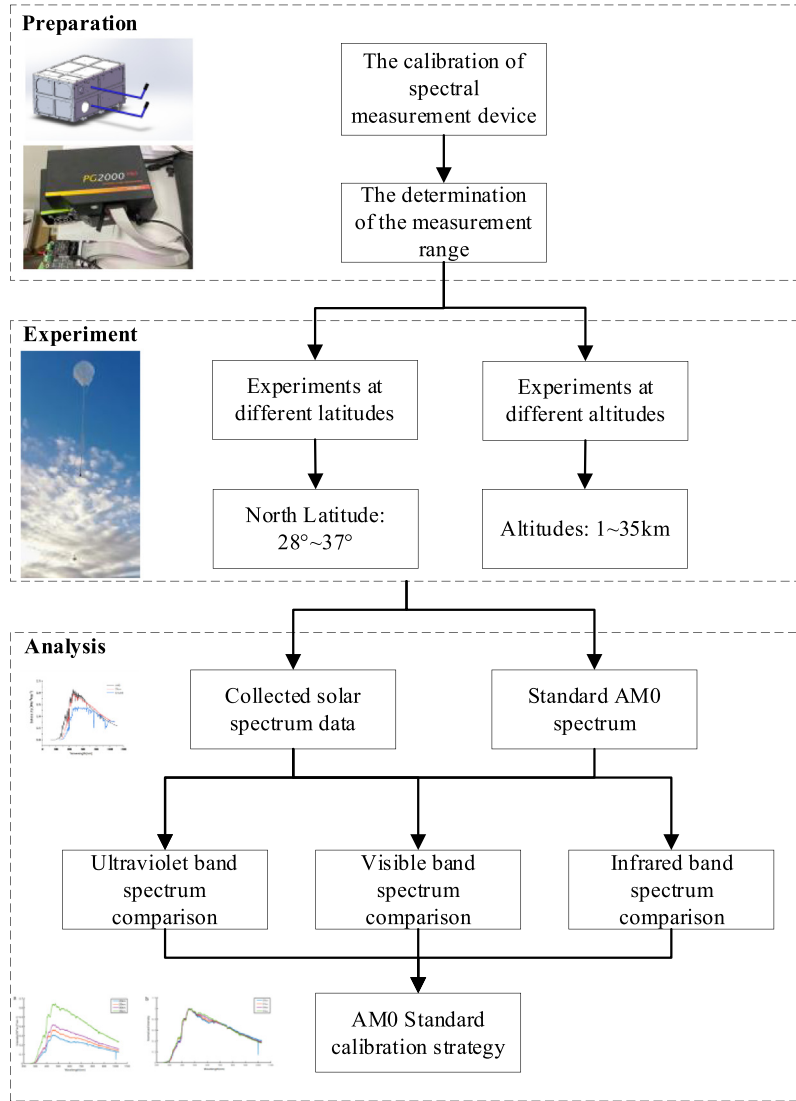


**Fig. 1.** The flowchart of this paper.

corrector and the fact that atmospheric scattering of solar radiation is minimal in near space, the spectrometer is not required to point directly towards the sun, which simplify the design of the system.

Spectrometers with CCD detectors can provide high rate of data acquisition and high sensitivity in a small, portable device [14]. For our spectrometer, the light enters from the probe, pass through fiber-optics, then through a polychromator which deflects light into different directions based on the wavelength, and finally reaching the CCD detector. The CCD detector has 2048 pixels, so the measured spectrum is made up of 2048 data points with different wavelengths. Due to errors in the manufacturing and assembly of the spectrometer, it is necessary to calibrate the spectrometer before using it [15].

The spectral measurement system (includes the cosine corrector) is calibrated by the National Institute of Metrology of China (NIM) to obtain the correction factors for the corresponding wavelength. The correction factors can be used to correct the collected data to obtain the value of the spectral irradiance. The principle of spectrometer calibration and data correction can be expressed as follows: if  $D$  is the spectral distribution of a known light source, and  $C$  is the spectrum of the light source measured by the spectrometer to be calibrated, and the relationship between

the measured spectrum (C) and the spectrum of the light source (D) is the spectral response factor k.

$$k = \frac{D}{C} \quad (1)$$

After the spectrometer was calibrated, the radiation energy distribution of an unknown light source can be measured and derived using Eq. (2).

$$D' = k \times C' \quad (2)$$

where,  $D'$  is the spectral distribution of the light source under test,  $C'$  is the measured value of the light source under test by the spectrometer.

## 2.2. Near space solar spectrum measurement method and platform

As shown in Fig. 2, the gondola that contains the payloads, flight control, communication system and power supply system are transported to an altitude of around 35 km using a high-altitude balloon with a volume of 30,000 m<sup>3</sup>. The high-altitude balloon maintains level flight at this altitude for 2–3 h, after which the rope cutter action separates the high-altitude balloon from the parachute, which carries the platform and payload safely down to the ground for recovery. The payloads carried for this test included a space solar cell calibration system and a spectral measurement system. The spectral measurement system works during the entire flight to measure the solar spectrum distribution at different altitude. Fig. 2 shows the spectrometry equipment and platform, where Fig. 2(a) shows the installation of the spectrometry unit and Fig. 2(b) shows the altitude of the high-altitude balloon platform and how it compares to other vehicles.

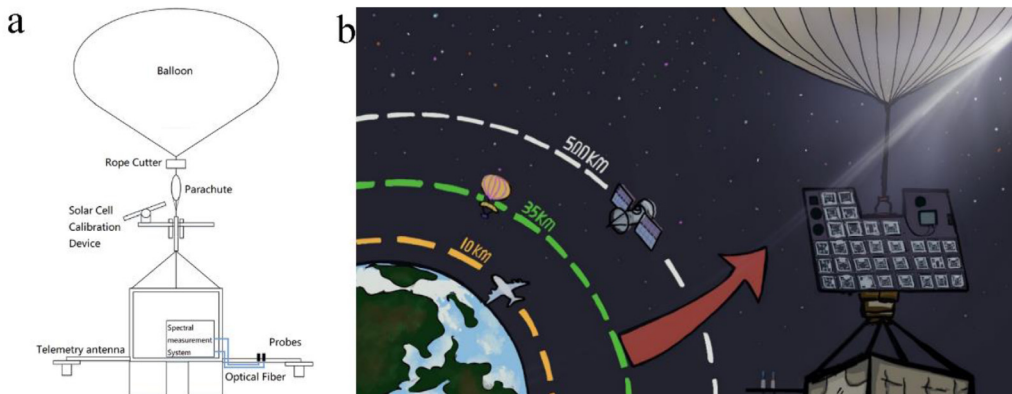


**Fig. 2.** Spectral measurement device and platform. (a) device installation (b) platform flight altitude.

## 2.3. Experiment plan

The flight test, named the Near Space Spectrometry Test, was conducted on 26 September 2021 in Da Qaidam, Qinghai Province. The balloon took off at 7:26 and ascended to an altitude of 35 km at 8:53, then maintain level flight for 162 min. Separation occurred at 11:35, followed by landing and recovery. The ground observation sites were chosen to be the launch site of the flight test, and two more sites in Tibet at the altitude of 4276 m and 5201 m, respectively. All of the observations for this experiment took place at altitudes in excess of 3000 m. Details of the observation sites are shown in Table 1.

**Table 1.** Detailed information of the sites of measurement.

No.	Location	Altitude/m	Latitude	Longitude	Date
1	Da Qaidam, Qinghai Province	20 000–35 000	37° 43'	95° 19'	2021.09.26
2	Da Qaidam, Qinghai Province	3243	37° 43'	95° 19'	2021.09.25
3	Shigatse, Tibet	4276	28° 12'	86° 33'	2022.05.23
4	Mount Qomolangma base camp	5201	28° 08'	86° 51'	2022.05.24

## 2.4. Data exploitation

Air Mass (AM) is commonly used to characterize the extent to which the atmosphere affects the reception of solar light in the region in which it is located [16]. The AM0 solar spectrum is the standard spectrum of sunlight striking the upper boundary of the atmosphere, before it has passed through any of it. After passing through the atmosphere, solar radiation collides with atmospheric molecules and particles and undergoes atmospheric scattering and atmospheric absorption, which change both its intensity and spectral distribution. The AM1.5G spectrum is the full spectrum of solar radiation, including direct and diffuse radiation, that reaches the test plane at an angle of 48.2° through 1.5 times the thickness of the atmosphere. In the near space environment at an altitude above 35 km, where the residual atmospheric is below 0.5% of that at sea level, the content of water vapors, ozone and dust is extremely low, the absorption and scattering of sunlight by atmospheric molecules is minimal and the solar radiation environment is already largely close to that of solar radiation in space.

The data acquired from our experiments is compared with the 2000 ASTM Standard Extraterrestrial Spectrum Reference E-490-00 spectrum. This is a standard AM0 spectrum, developed by the American Society for Testing and Materials (ASTM) based on data from multiple observations, and is widely used in related fields. The data collected at different altitude and different time of the day is also compared to show the impact of different level of atmospheric absorption with respect to the change in height and solar altitude.

Different atmospheric components absorb radiation at different wavelengths of the solar spectrum, and deviation from AM0 spectrum is mainly due to the absorption of solar radiation by ozone, oxygen, water vapor, carbon dioxide and other molecules in the atmosphere [12,17]. The earth atmosphere only contains small amount of ozone but its absorption of solar radiation is strong, with a strong absorption band at 200–300 nm (Hartley–Huggins Band) and a broad absorption band near 600 nm (Chappuis band). Water vapor absorbs far-infrared radiation at 0.930–0.285  $\mu\text{m}$ , and solar radiation can be attenuated by 4%–15% due to the absorption of water vapor; while the atmosphere contains large amount of nitrogen and oxygen, only oxygen can weakly absorb solar radiation, and the main absorption bands are around 200 nm, correspond to the Schumann–Lunger band and the Hertzberg band, as well as a narrow absorption band around 690 and 760 nm. Carbon dioxide absorbs near 4.3  $\mu\text{m}$  and has little effect on the overall solar radiation.

For the application of balloon-based space solar cell calibration, it is more important to have spectral distribution in those band where the solar cells were the most sensitive. For the emerging multi-junction space solar cells and perovskite solar cells, the response of their sub-cells to lights with different wavelengths is more complex than that of the traditional single-junction solar cells [18–21]. So, we divide the spectrum into ultraviolet (UV) band, visible (VIS) band and infrared (IR) band and further analyze the difference between spectrum from our measurements (especially the spectrum at 35 km altitude) and standard AM0 spectrum.

## 3. Result and discussion

### 3.1. Experiments at different altitudes

Fig. 3 shows the upper atmospheric solar spectrum collected at 11:32 during the level flight phase of the flight test on September 26th, 2021 and compared it with AM0 spectrum. Fig. 3(a) shows the comparison between the

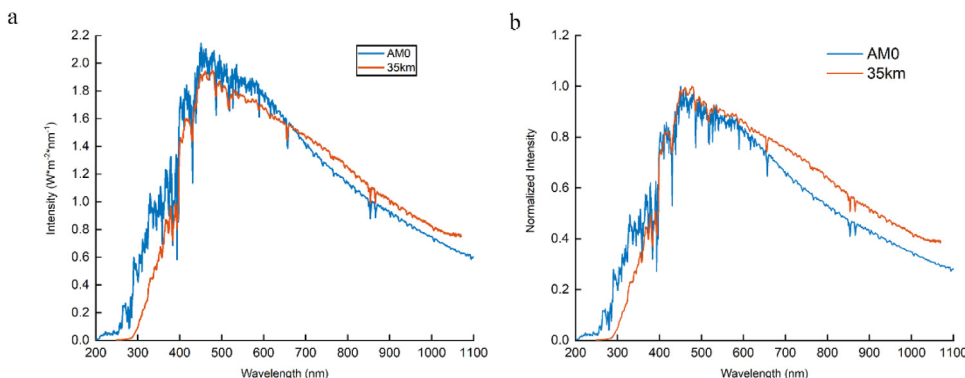


Fig. 3. Comparison between solar spectrum at 35 km altitude and standard AM0 spectrum. (a) original data (b) normalized data.

solar spectrum at a zenith angle of 0 degrees and the standard spectrum, and it can be seen that the maximum intensity of the AM0 spectrum occurs at 451 nm, and the correspond intensity is  $2.12 \text{ W}\cdot\text{m}^{-2}\cdot\text{nm}^{-1}$ ; the maximum intensity of the solar spectrum from our measurement at 35 km altitude occurs at 478 nm, and the correspond intensity is  $1.95 \text{ W}\cdot\text{m}^{-2}\cdot\text{nm}^{-1}$ , 92% of the maximum intensity of the AM0 spectrum. Although the spectrometer's probe is equipped with a cosine corrector, but the probe was not placed directly toward the sun in our experiment. As a result, the light intensity from this measurement will surely below the intensity of the direct solar spectrum, so this result was as expected.

In order to focus on the energy distribution of the solar radiation, the intensity was normalized and shown in Fig. 3(b). It is clear that the spectral energy distribution at 35 km is very similar to the AM0 spectrum, especially at 378–618 nm in the VIS band. Integration of the intensity of wavebands were performed and the results are shown in Table 2. From Table 2, it can be seen that in the UV band ranging from 250 nm to 400 nm, the intensity of the solar spectrum at 35 km is lower than that of the AM0 spectrum. In the VIS band ranging from 400 nm to 780 nm, the two spectrums have very similar intensity. And in the near-infrared band exceed 780 nm, the intensity of the solar spectrum at 35 km is slightly greater than that of the AM0 spectrum. Above the stratosphere the absorption of UV radiation is mainly caused by oxygen and ozone, and the absorption and scatter from atmospheric components is mostly at the infrared and UV band and is almost transparent to VIS band.

**Table 2.** Comparison between normalized spectrum at 35 km and standard AM0 spectrum.

Band	35 km integrated intensity/ $\text{W}\cdot\text{m}^{-2}$	AM0 integrated intensity/ $\text{W}\cdot\text{m}^{-2}$	Relative intensity (35 km/AM0)
UV (250–400 nm)	30.4	48.3	62.9%
VIS (400–780 nm)	316.2	294.6	107.4%
IR (780–1070 nm)	144.9	118.7	122.1%

**Table 3.** Original spectrum at 35 km and ground.

Band	35 km integrated intensity/ $\text{W}\cdot\text{m}^{-2}$	Ground (3.2 km) integrated intensity/ $\text{W}\cdot\text{m}^{-2}$	Relative intensity (Ground/AM0)	Relative intensity (35 km/AM0)
UV (250–400 nm)	59.3	27.3	26.3%	57.2%
VIS (400–780 nm)	616.2	474.3	75.1%	97.6%
IR (780–1070 nm)	282.3	252.0	99.0%	110.9%

Acquiring the solar spectrum on 25 September 2021 at 16:30 during the ground test phase (corresponding to the same zenith angle of 0 degrees) and compare it with the 35 km solar spectrum and the reference AM0 spectrum, shown in Fig. 4. Compared to the AM0 solar spectrum and the 35 km solar spectrum at the upper atmospheric boundary, the maximum intensity of the surface solar spectrum at this time occurs near 480 nm, with an intensity of  $1.39 \text{ W}\cdot\text{m}^{-2}\cdot\text{nm}^{-1}$ . This peak intensity is 65.6% of the AM0 spectrum and 71.2% of the 35 km solar spectrum, with little variation in intensity throughout the visible band.

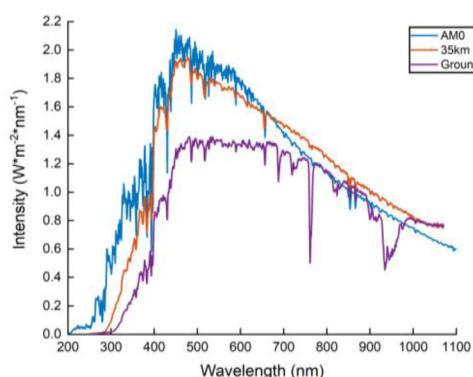


**Fig. 4.** Comparison of solar spectrum at ground (3243 m), 35 km altitude and standard AM0 spectrum.

From the ground-based solar spectra observed in this experiment, the absorption bands of ozone are around 376 nm, the absorption bands of oxygen are around 654.2 nm, 688.9 nm and 763.3 nm, and the absorption bands of water vapor are around 722.6 nm, 823.5.8 nm and 936.0 nm. The solar spectrum at an altitude of 35 km is almost free of water vapor and oxygen absorption from atmospheric absorption, and there is only weak ozone absorption.

**Table 3** shows the integrated intensity of original spectrum (without normalization) from our measurements at 35 km and 3.2 km altitudes, and the relative intensities of these data to standard AM0 spectrum. For the unnormalized data, the intensity integration ratio of 35 km to AM0 in the VIS band is 97.6%, which is very similar. In the UV band at 250–400 nm, the 35 km data are more accurate, and in the near IR band at 780–1070 nm, the ground data are better. Note that due to the limited range of our instrument, much of the IR spectrum has not been taken into account.

The solar spectrum at different altitudes during the ascent phase of the flight was collected from 8:15 to 8:53, in 38 min, as shown in **Fig. 5(a)**. With the increase of altitude, the spectral intensity of the full waveband increase. It can be seen that the intensity in UV band increase the most significant, this is due to the fact that ozone in the atmosphere is mainly exist in the altitude range of 20–50 km, and ozone has a strong absorption on UV light, so the increase in altitude reduces the absorption by ozone in the UV spectrum. Also, the solar spectrum in the visible VIS band (500–650 nm) increases gradually with the increase in altitude. Since the atmosphere has only slight absorption in this band, it is possible that this is due to the increase in solar altitude angle. And in the near-infrared region the intensity of the spectrum decreases slightly, this maybe be caused by the decrease of reflected light from clouds and other objects in the infrared band as altitude increases.

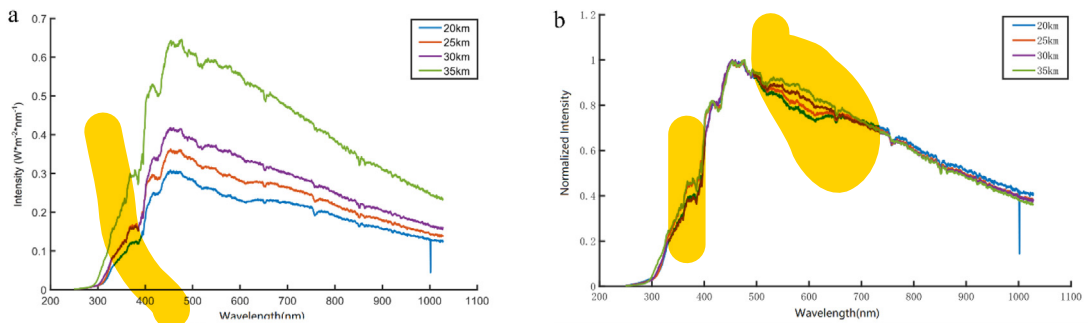


**Fig. 5.** Spectrum measured during the ascent phase of the flight. (a) original data (b) normalized data.

**Fig. 6** shows the solar spectrums between 9:00 and 11:30 at a 30-min interval. All these data were gathered during the level flight phase. It shows more clearly that as the altitude angle of the sun increases, the energy in all bands of the solar spectrum increases, and the rate of these increases gets smaller as it approaches midday. Also, the absorption lines were more clearly seen.

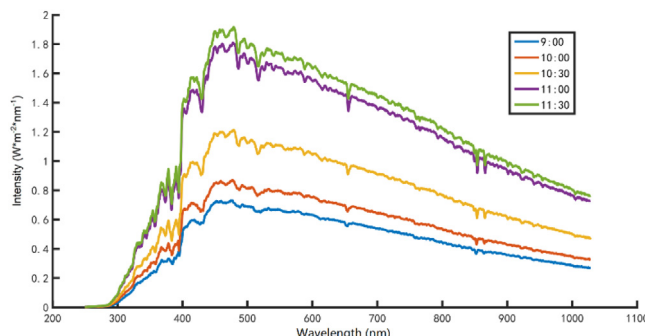


**Fig. 6.** Solar spectrum of different time in the level flight phase.

### 3.2. Experiments at different latitudes and altitudes

**Fig. 7** shows the solar spectrum respectively collected in Xigaze (Tibet autonomous region), Mount Qomolangma base camp (Tibet autonomous region) and Da Qaidam (Qinghai province), shown as **Table 1**. In **Fig. 7(a)**, the X-axes shows the wavelength, the Y-axes shows the solar radiation intensity. The solar spectrum curves of Xigaze (4300 m), Mount Qomolangma base camp (5200 m), Da Qaidam (3200 m) and Da Qaidam (35 km) are respectively marked in green, purple, blue, and red. While in **Fig. 7(b)**, the Y-axes shows the solar radiation intensity after normalization, the solar spectrum curves of Xigaze (4300 m), Mount Qomolangma base camp (5200 m) are marked in red and blue.

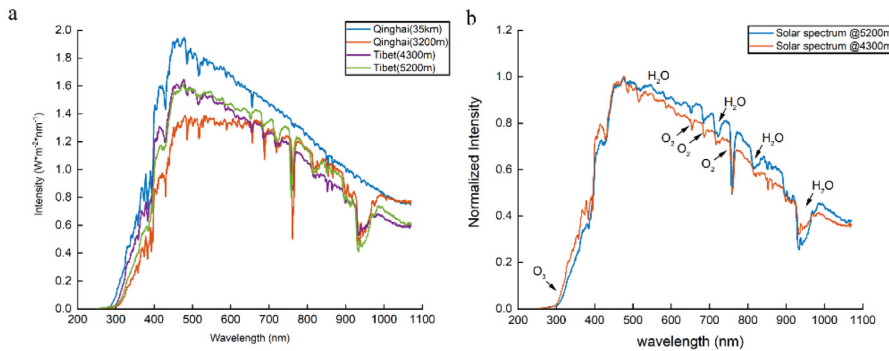


**Fig. 7.** Spectrum measured at different latitudes and altitudes. (a) Qinghai and Tibet (b) Tibet. . (For interpretation of the references to color in this figure legend, the reader is referred to the web version of this article.)

In **Fig. 7(a)**, the maximum solar spectral intensity of Qinghai and Tibet appeared at 477 nm, and the values are  $1.615 \text{ W} \cdot \text{m}^{-2} \cdot \text{nm}^{-1}$  and  $1.64 \text{ W} \cdot \text{m}^{-2} \cdot \text{nm}^{-1}$  respectively, while the maximum spectral intensity of AM1.5G appeared at 495 nm,  $1.62 \text{ W} \cdot \text{m}^{-2} \cdot \text{nm}^{-1}$ , which means that the maximum spectral intensity and band of the two places are close to AM1.5G. In **Fig. 7(b)**, the sunken of the curves is due to the absorption of gas. The absorption band of ozone is in the ultraviolet band, and there is a sharp decline at about 383.2 nm. The absorption band of oxygen spreads at about 652.3 nm, 685.5 nm, 759.0 nm, and the absorption band of water vapor spreads at about 723.9 nm, 819.3 nm, 932.8 nm.

The comparison of spectral integrated intensity at different latitudes and altitudes is shown in **Table 4**. In Qinghai (35 km), the spectral intensity of UV, VIS and IR are 59.3, 616.2, and 282.3 respectively, which are much larger than that of Qinghai (3.2 km), Tibet (4.3 km) and Tibet (5.2 km), which means that the solar intensity has significant attenuation since the absorption of gas.

**Table 4.** Comparison of spectral integrated intensity at different latitudes and altitudes.

Band	Qinghai (35 km) integrated intensity/W·m⁻²	Qinghai (3.2 km) integrated intensity/W·m⁻²	Tibet (4.3 km) integrated intensity/W·m⁻²	Tibet (5.2 km) integrated intensity/W·m⁻²
UV (250–400 nm)	59.3	27.3	46.8	36.4
VIS (400–780 nm)	616.2	474.3	521.2	530.6
IR (780–1070 nm)	282.3	252.0	222.4	231.8

### 3.3. The results

Through the analysis of experiment data of solar spectrum at different latitudes and AM0 standard solar spectral, the conclusion can be obtained that in different latitudes ( $28^\circ$  and  $37^\circ$ ), because of the absorption of gas (such as oxygen, water vapor, ozone), the solar spectral distribution on the ground (lower than 5.2 km) differs greatly from that of AM0, which means that the ground is not suitable for AM0 standard solar cell calibration.

Comparing the experiment data of solar spectrum at different altitudes and AM0 standard solar spectral. After normalization, we find that the values are differs greatly in 350 nm–400 nm and 500 nm–600 nm bands when the height is over 20 km. With the elevation rising, the distribution of collected experiment solar spectral and AM0 standard solar spectral tend to be consistent, which means that AM0 standard solar cell calibration is suitable. Specially, at an altitude of 35 km, the measured values of VIS band (400 nm~780 nm) after normalization are nearly identical with AM0 standard solar spectral.

#### 4. Conclusion

In this paper, the experiments for measuring the solar spectrum at different latitudes and altitudes are taken to obtain a suitable AM0 Standard solar cell calibration strategy. This is the first report on measurements and analysis of solar spectrum at such a wide range of altitudes, and we find that the spectral distribution at 35 km is almost equivalent to that of AM0, which supplies a suitable AM0 Standard solar cell calibration strategy with high altitude balloon flights. Comparing the measurement spectrum with AM0 standard spectrum, the following conclusions can be drawn:

- The solar spectrum at the altitude of 35 km above sea level in near space is highly similar to the solar spectrum outside the atmosphere, especially in the visible band.
- In the ultraviolet band, there are some differences between the solar spectrum at 35 km and the AM0 spectrum, which may be related to the strong absorption of ultraviolet radiation by atmospheric ozone.
- In the altitude range of 20–35 km, the intensity of the ultraviolet band spectrum varies more significantly, while the intensity of the other bands does not. This is due to the decrease in total atmospheric ozone above as altitude increases, and the absorption in the ultraviolet band decreases significantly.
- In terms of spectral energy distribution, the solar spectrum in near space is very close to the AM0 spectrum, while the ground base solar spectral measurement yield result with much more difference. Spectral distribution observations and space solar cell tests in the near space environment can replace, to some extent, the use of spacecraft for similar experiments. Also, our experiment shows that using high-altitude balloons to obtain solar reference spectra is feasible.

#### Declaration of competing interest

The authors declare that they have no known competing financial interests or personal relationships that could have appeared to influence the work reported in this paper.

#### Data availability

Data will be made available on request

#### Acknowledgments

This work was funded by the Scientific Experimental System in Near Space of Chinese Academy of Sciences (XDA17020304)

#### References

- [1] Yang W. Calibration of standard solar cells for aerospace. *Aerosp China* 1983;05:14–7+22.
- [2] Dang X. Brief analysis of solar cell calibration technology and standard for aerospace. *Aerosp Stand* 2016;04:12–4.
- [3] Hoheisel R, Wilt D, Scheiman D, Jenkins P, Walters R. AM0 solar cell calibration under near space conditions. In: Proceedings of the 2014 IEEE 40th photovoltaic specialist conference. Denver: IEEE; 2014.
- [4] Zhang Y, Yuan Y, Tang H. Primary investigation of the AM0 solar cell space calibration. *J Astronaut Metrol Meas* 2010;30(01):28–32.
- [5] Reb LK, Böhmer M, Predeschly B, Grott S, Weindl CL, Ivandekic GI, Guo R, Dreizigacker C, Gernhäuser R, Meyer A, Müller-Buschbaum P. Perovskite and organic solar cells on a rocket flight. *Joule* 2020;4(9):1880–92.
- [6] Tu Y, Xu G, Yang X, Zhang Y, Li Z, Su R, Luo D, Yang W, Miao Y, Cai R, Jiang L, Du X, Yang Y, Liu Q, Gao Y, Zhao S, Huang W, Gong Q, Zhu R. Mixed-cation perovskite solar cells in space. *Sci China Phys Mech Astron* 2019;62(7):1–4.
- [7] Zoutendyk JA. Space calibration of standard solar cells using high-altitude balloon flights. *J Spacecr Rockets* 1965;2(3):399–404.
- [8] Bailey SG, Snyder DB, Jenkins P, Scheiman DA, Mueller RL, Pichetto V, Emery K, Baur C, Messenger SR, Goodbody C. Standards for space solar cells and arrays. In: Proceedings of the seventh european space power conference. Stresa, ESA; 2005.

- [9] Anspaugh BE, Mueller RL, Weiss RS. Results of the 2000 JPL balloon flight solar cell calibration program. *Natl Aeronaut Space Adm Jet Propuls Lab* 2001;20–5.
- [10] Xu Z, Xu G, Luo Q, Han Y, Tang Y, Miao Y, Li Y, Qin J, Guo J, Zha W, Gong C, Lu K, Zhang J, Wei Z, Cai R, Yang Y, Li Z, Ma CQ. In situ performance and stability tests of large-area flexible polymer solar cells in the 35 km stratospheric environment. *Natl Sci Rev* 2022.
- [11] Kambezidis HD, Melas LD, Kampezidou DH, Psiloglou BE. Effect of tropospheric nitrogen dioxide on incoming solar radiation. *J Sol Energy Res Updates* 2015;2(1):14–7.
- [12] Wang C. Inversion of SO<sub>2</sub> and O<sub>3</sub> column concentration based on observed solar spectrum. Nanjing University of Information Science and Technology; 2017.
- [13] Cordero RR, Damiani A, Seckmeyer G, Jorquera J, Caballero M, Rowe P, Ferrer P, Mubarak R, Carrasco J, Rondanelli R, Matus M, Laroze D. The solar spectrum in the Atacama desert. *Sci Rep* 2016;6(1):22457.
- [14] Gaigalas AK, Wang L, He HJ, DeRose P. Procedures for wavelength calibration and spectral response correction of CCD array spectrometers. *J Res Natl Inst Stand Technol* 2009;114(4):215–28.
- [15] Belyaev YV, Rogovets AV, Khomitsevich AD, Tsikman IM. Portable PVS-02 spectrometer for transfer of the spectral radiance scale in the 0.4–2.5  $\mu\text{m}$  range. *J Appl Spectrosc* 2010;77(5):722–7.
- [16] Xu G, Tang Y, Li Z, Cai R, Jiang L, Miao Y. Research on key technology of solar cell high altitude balloon calibration. *J Sol Energy* 2021;42(10):94–104.
- [17] Gelsor N, Juan L, Wangmo T, Tunzhup L, Gelsor N. Measurements on solar energy resources in the Mt. Everest Region. *Am J Phys Appl* 2021;9(1):1–9.
- [18] Garcia J, Socolovsky H, Plá J. On the spectral response measurement of multijunction solar cells. *Meas Sci Technol* 2017;28(5):055203.
- [19] Tu Y, Wu J, Xu G, Yang X, Cai R, Gong Q, Zhu R, Huang W. Perovskite solar cells for space applications: progress and challenges. *Adv Mater* 2021;33(21):2006545.
- [20] Marangi F, Lombardo M, Villa A, Scotognella F. New strategies for solar cells beyond the visible spectral range. *Opt Mater: X* 2021;11:100083.
- [21] Yang JW, Jeong RH, Boo JH. Enhancement of UV-light harvesting in perovskite solar cells by internal down-conversion with Eu-complex hole transport layer. *Energy Rep* 2022;8:214–22.